

CO₂ Absorption in a Lab-Scale Fixed Solid Bed Reactor: Modelling and Experimental Tests

Franco Donatini, Michele Landi, Massimo Schiavetti and Juri Riccardi*
Enel Produzione Ricerca,
via Andrea Pisano 120, 56122 Pisa, Italia
E-mail: juri.riccardi@enel.it

Roberto Gabbrielli
Università di Pisa, Dipartimento di Energetica,
Via Diotisalvi 2, 56126 Pisa, Italia

Abstract

The CO₂ absorption in a lab-scale fixed solid bed reactor filled with different solid sorbents has been studied under different operative conditions regarding temperature (20-200°C) and input gas composition (N₂, O₂, CO₂, H₂O) at 1bar pressure. The gas leaving the reactor has been analysed to measure the CO₂ and O₂ concentrations and, consequently, to evaluate the overall CO₂ removal efficiency. In order to study the influence of solid sorbent type (i.e. CaO, coal bottom ash, limestone and blast furnace slag) and of mass and heat transfer processes on CO₂ removal efficiency, a one-dimensional time dependent mathematical model of the reactor, which may be considered a Plug Flow Reactor, has been developed. The quality of the model has been confirmed using the experimental results.

Keywords: CO₂ absorption, solid sorbents, mathematical modelling, fixed solid bed reactor

1. Introduction

The greenhouse effect is the warming of the Earth's surface and of the lower atmosphere due to a trapping of the infrared radiation emitted by ground, vegetation and oceans in the atmosphere. This phenomenon is produced by the presence in the atmosphere of particular gases, i.e. nitrous oxide, water vapour, methane, chloro-fluorocarbons, and carbon dioxide. These gases are also known as greenhouse gases (GHG).

The increase of the GHG emissions, especially CO₂ (estimated at 26000 Mton/year), caused by human activity and the widespread use of fossil fuels (coal, oil and natural gas), seems to intensify the greenhouse effect and in the next 30-40 years severe and critical climatic changes may result (Bacci 2001, Sigman and Boyle 2000, Davison, et al. 2001).

In December 1997 the Kyoto Protocol pointed out the international objectives to contain the GHG emissions, especially CO₂. In the Kyoto Protocol developed countries agreed to reduce their emissions by 5.2% below 1990 levels, although, at the present, this protocol has not yet been ratified by the necessary minimum

number of participants. In particular, among the countries that have signed the Kyoto Protocol an agreement on how to calculate the emission reductions does not exist.

In the power generation sector the main methods that have been proposed for the capture and controlled release of CO₂ are based on one of the following chemical or physical processes (Davison et al. 2001):

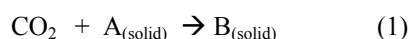
- i) absorption using liquid substances, such as alkanolamines, especially MEA (mono-ethanolamine) and DEA (diethanolamine);
- ii) adsorption using solid adsorbents, such as zeolites, activated carbon, alumina and silica gel;
- iii) cryogenic separation at very low temperature;
- iv) membrane separation using many different membranes (such as porous membranes, polymeric membranes and zeolites).

About the CO₂ storage, one of the most promising technologies among those proposed, is the CO₂ injection in the oceans' depths (Ormerod et al. 2002, Giavarini and Maccioni 2001, Liro et

* Author to whom correspondence should be addressed.

al. 1999). In this case, in order to minimise the environmental impact, the CO₂ has to be injected at depths of at least 1500 m. However, for the technologies cited above the costs are high and several significant technical problems remain unsolved (Reeve, 2001).

The CO₂ chemical absorption in a fixed solid bed reactor discussed in this paper could represent another interesting method both for the capture and storage of the CO₂ from flue gas at thermal power plants. Moreover, this technique could be economically advantageous if it is possible to use waste solid materials, such as limestone, bottom ash, blast furnace slag, etc. CO₂ absorption inside solid sorbents, such as CaO and/or MgO, is based on the carbonation reactions and the process can be represented as follows:



where A is CaO and/or MgO and B is CaCO₃ and/or MgCO₃. The carbonation reactions are exothermic and the produced carbonates are thermodynamically stable compared with the reagents ($\Delta G^\circ = -130.2$ kcal/mol in the reaction with CaO and $\Delta G^\circ = -75.2$ kcal/mol in the reaction with MgO). The inverse reactions are consistent only at high temperatures (for a CO₂ partial pressure equal to 1 bar, $T > 800^\circ\text{C}$ for the CaCO₃ and $T > 500^\circ\text{C}$ for the MgCO₃) and, at ambient conditions of temperature and pressure, the calcium and magnesium carbonates can be considered a safe option for CO₂ storage.

In order to study non-catalytic gas-solid reactions, many models have been developed. The following four models are widely used in the literature (Gupta et al. 2001, Levenspiel 1978):

- i) grain model;
- ii) pore model;
- iii) percolation model;
- iv) progressive conversion model.

As discussed in the References (Gupta et al. 2001, Bhatia and Perlmutter 1983, Mess et al. 1999, Dedman and Owen 1962) the carbonation reaction is initially fast and chemically controlled. However, as a consequence of the increasing conversion, further reaction can take place only through CO₂ diffusion in the CaCO₃ or MgCO₃ layer and the reaction does not go to complete conversion of the solid.

Extensive work (Gupta et al. 2001, Mess et al. 1999, Dedman and Owen 1962) about the carbonation kinetic has been performed, but the values proposed for the reaction rate are quite different and a complete agreement does not exist. In this paper further investigation on the effective carbonation reaction rate in different solid sorbents is performed.

The outline of this paper is as follows: In section 2 the experimental activity and the main experimental results obtained are described. In section 3 a mathematical modelling developed in order to describe the CO₂ absorption inside the reactor based on a progressive conversion simplified model is described. In section 4 the comparison between experimental and model results is made. Finally, some conclusions and remarks are reported.

2. Experimental

2.1 Description of the apparatus and experimental procedure

The experimental tests were performed in a lab-scale fixed bed reactor made up of Pyrex glass (Figure 1). The reactor, with cylindrical geometry (diameter = 0.1 m, length = 1.2 m), was equipped with three mass flow controllers and an impinger filled with water in order to mix the input gases at the typical thermal power plant flow gas composition. The impinger was used to saturate the gaseous mixture of nitrogen, oxygen and carbon dioxide with water vapour at a controlled temperature. The impinger was designed to assure the complete water saturation at 25°C. The inlet gas composition is shown in TABLE I. The reactor was coated with heating tapes and cords in order to keep the internal temperature in a range between 20 and 200°C. Furthermore, an electronic temperature controller (Cole-Parmer Instruments Co.) was used to set and keep the process temperature constant. The inlet and outlet gas composition were analysed using a Siemens Ultramat Analyzer equipped with a electrochemical cell detector for the measurement of O₂ concentration and a non dispersive infrared detector for the measure of CO₂ concentration. Mass flow controllers and gas analysers were connected to an electronic data acquisition system. The CO₂ absorption in the reactor was studied using four different solid sorbent materials: calcium oxide (CaO), compact limestone, bottom ash from coal-fired thermal power plant and blast furnace slag.

TABLE I. INPUT GAS COMPOSITION

	% by volume
Oxygen (O ₂)	2.6
Nitrogen (N ₂)	82.2
Water vapour (H ₂ O)	2.5
Carbon dioxide (CO ₂)	12.7
Total flow (litres/min)	1.0

The solids were milled until particles with diameters in the range of 0.1-3 mm were obtained. For each solid sorbent both the granulometric distribution and the chemical composition were measured using a scanning electronic microscope (SEM) coupled with an energy-dispersive X-ray analyser.

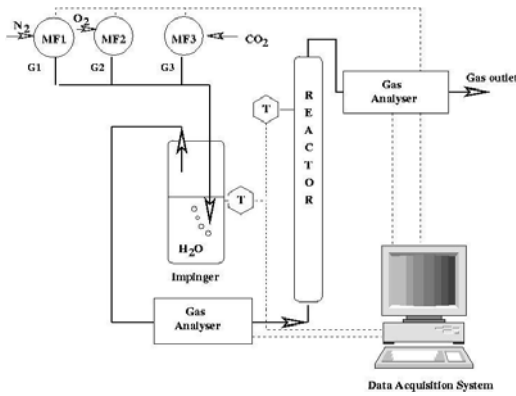


Figure 1. Scheme of the experimental apparatus, where MF1, MF2 and MF3 are mass flow controllers and T are thermocouples

Finally, the chemical and physical properties of the solid sorbents used in the experimental tests are reported in TABLE II.

TABLE II. CHEMICAL AND PHYSICAL PROPERTIES OF SOLID SORBENTS

	Calcium oxide	Bottom ash	Blast furnace slag	Limestone
Bulk density [kg/m ³]	1000	1666	764	1069
True density [kg/m ³]	3250	2362	1888	2780
Average diameter [mm]	3	0.30	0.86	0.49
Porosity [-]	0.7	0.29	0.60	0.62
<i>Chemical composition</i>				
Na	-	0.6	0.8	0.05
Mg	-	0.9	8.3	0.2
Al	-	15.2	6.7	0.1
Si	-	25.5	17.0	0.2
S	-	-	1.0	-
Cl	-	-	0.3	-
K	-	1.3	0.3	-
Ca	71.4	3.7	23.4	28.4
Fe	-	4.3	-	-
Ti	-	0.8	-	-
C	-	-	-	12.9
O	28.6	47.7	42.0	58.3
<i>Composition of oxide</i>				
Na ₂ O	-	0.8	1.1	0.07
MgO	-	1.5	13.7	0.33
Al ₂ O ₃	-	28.6	12.7	0.19
SiO ₂	-	54.7	36.5	0.43
SO ₃	-	0.1	2.5	-
K ₂ O	-	1.6	0.4	-
CaO	100	5.2	32.8	39.8
TiO ₂	-	1.4	-	-
Fe ₂ O ₃	-	6.1	-	-
Theoretical maximum CO ₂ uptake [kgCO ₂ /kg sorbent]	0.78	1.31	1.12	0.33

The theoretical maximum CO₂ uptake has been calculated using the oxides' composition. The oxygen content is obtained by the difference.

2.2 Experimental procedure

Each experimental test was carried out by first filling homogeneously the vertical reactor with the fresh solid sorbent. For each type of sorbent, the CO₂ absorption was studied at three different temperatures: low temperature (25°C),

medium temperature (100°C) and high temperature (200°C). In each test the inlet gas composition was set up to the values in TABLE I using the mass flow controllers and the impinger as shown in Figure 1. The gas leaving the reactor was analysed using the gas analyser, and the CO₂ concentration was recorded by the data acquisition system. The outlet gas flow rate was further checked using a high precision flowmeter.

2.3 Experimental results

In each experimental test the CO₂ absorption rate $v(t)$ at the generic time t was determined according the following relation:

$$v(t) = C_o Q_o - Q_H(t) C_H(t) \quad (2)$$

where $Q_H(t)$ and $C_H(t)$ are the gas flow rate and the CO₂ concentration measured at the reactor outlet, respectively. The average value of the rate constant per surface reaction k_A was calculated as:

$$k_A = \frac{1}{t_r} \int_0^{t_r} \frac{1}{\pi d^2 n_o \theta (1-\varepsilon) S H \bar{C}(t)} v(t) dt \quad (3)$$

where $\bar{C}(t)$ was the average CO₂ concentration inside the reactor at the generic time t . This equation has been obtained by the authors via a mass balance of the CO₂ absorbed inside the reactor on the basis of experimental data; the only hypothesis assumed is that it is reasonable to use an average CO₂ concentration in the reactor at each time. Finally, the average integral method on the values of k_A obtained at each time was applied. In the first approximation, $\bar{C}(t)$ was estimated as the arithmetic average between the inlet and outlet CO₂ concentration:

$$\bar{C}(t) = (C_o + C_H(t))/2$$

The CO₂ specific absorption $A(t)$ as a function of time was then obtained according to the formula:

$$A(t) = \frac{\text{weight of the CO}_2 \text{ absorbed until time } t}{\text{weight of the sorbent inside the reactor}}$$

$$A(t) = 1/M \int_0^t v(t) dt \quad (4)$$

The average value of the CO₂ removal efficiency E was calculated as follows:

$$E = 1 - \frac{\int_0^{t_r} Q_H(t) C_H(t) dt}{t_r Q_o C_o} \quad (5)$$

In Figures 2, 3 and 4 the CO₂ specific absorption for each sorbent investigated is reported at three temperatures.

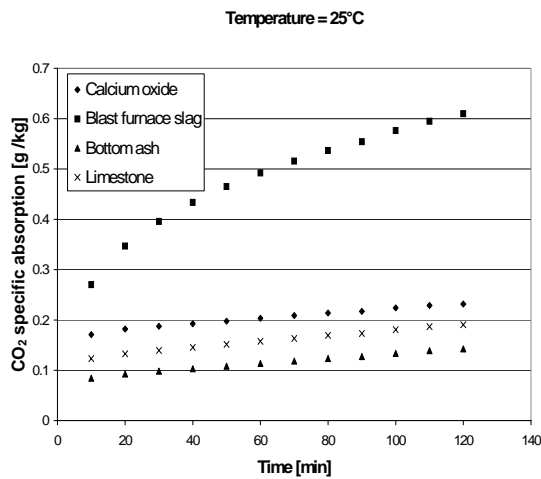


Figure 2. CO_2 specific absorption for the different solid sorbents used at $T = 25^\circ\text{C}$

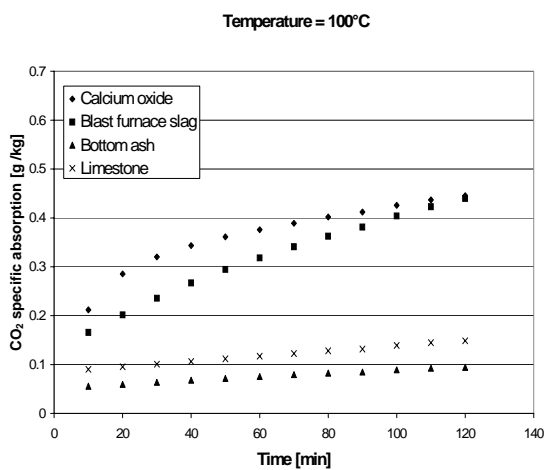


Figure 3. CO_2 specific absorption for the different solid sorbents used at $T = 100^\circ\text{C}$

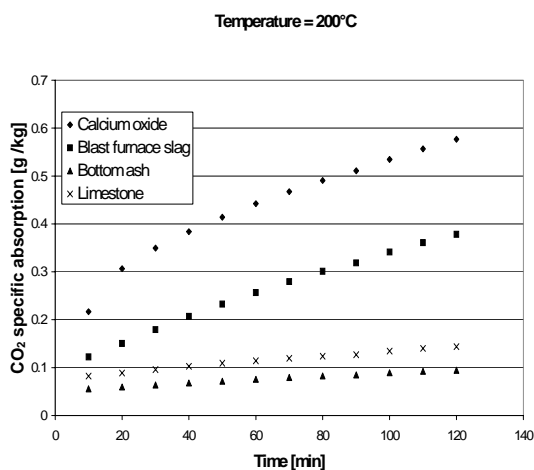


Figure 4. CO_2 specific absorption for the solid sorbents used at $T = 200^\circ\text{C}$

For the bottom ash and the limestone the CO_2 absorption is very small and is almost constant with the temperature. Consequently, for these sorbents it may be reasonably supposed that no chemical reaction takes place. For these two solid sorbents, the CO_2 average removal efficiency measured, in the range of temperature investigated, is between 4% and 7% as shown in TABLE III. Probably the weak CO_2 adsorption processes on the surface of the particles. The CO_2 absorption with CaO increases considerably with the temperature: the average CO_2 removal efficiency increases from 8% at $T = 25^\circ\text{C}$ to 20% at $T = 200^\circ\text{C}$ as shown in TABLE III. In any case the value of the CO_2 specific absorption is very low: 0.6 gr of CO_2 absorbed per kg of CaO.

In Figure 5 the Arrhenius plot for the gas-solid heterogeneous reaction between CaO and CO_2 is reported: the activation energy and pre-exponential factor are estimated to be about 15.2 kJ/mol and $4.6 \cdot 10^{-5}$ m/s, respectively.

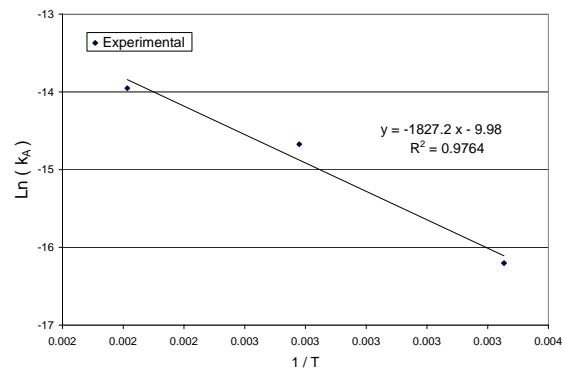


Figure 5. Arrhenius plot for the CaO-CO_2 reaction, where R^2 is the correlation coefficient

The blast furnace slag shows an opposite trend with respect to the CaO since the absorption decreases when the temperature increases: the CO_2 average removal efficiency varies from 14% at $T = 20^\circ\text{C}$ to 10% at $T = 200^\circ\text{C}$, as shown in TABLE III. A possible explanation of this behaviour could be the moisture contained in the blast furnace slag (about 1%) in comparison with the other sorbents, which have a very low moisture content (lower than 0.1%). In the blast furnace slag, at temperatures below 100°C , the moisture contributes to the CO_2 absorption, while this adjunctive effect in the other sorbents investigated is absent.

Moreover, in each experimental test it was observed that the outlet CO_2 concentration, after a certain time (depending on the sorbent and the temperature), did not change any more with time.

This is clearly shown in *Figure 7* where the CO₂ concentration reaches a stationary value after a brief transitory time. In this *Figure* the time $t=0$ s corresponds to the time at which the gas enters the reactor and the transitory time is comparable to the time $t_c=H/u$ required by the gas to cross the whole reactor (about 2-4 min, depending both on the reactor temperature and on the interparticles voidage). Therefore, in order to characterize the CO₂ removal efficiency when the reactor reaches a stationary condition, as an alternative to the definition (5), we have introduced the parameter E_s , which is defined as follows:

$$E_s = 1 - \frac{\int_{t_0}^{t_r} Q_H(t) C_H(t) dt}{(t_r - t_0) Q_0 C_0} \quad (6)$$

where t_0 is the time necessary at the reactor to reach stationary conditions. The CO₂ stationary removal efficiency E_s is a parameter that better describes the sorbent behaviour in experimental tests carried out over a long time. For all sorbents the CO₂ removal efficiencies calculated using equation (6) are considerably less than those obtained by equation (5) and are shown in TABLE III.

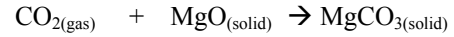
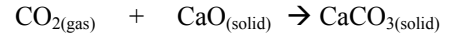
3. Mathematical Model

3.1 Description of the model

In order to evaluate the influence of solid sorbents, type, mass and heat transfers on the absorption process and on the CO₂ removal efficiency in the reactor, a specific mathematical model was developed. In the model the reactor was considered as a one-dimensional unsteady isothermal Plug Flow Reactor. Any kind of backmixing and longitudinal diffusion were neglected and each fluid element spent the same time in the reactor. Therefore, at each time, the concentration and the temperature of the CO₂ in the reactor are flat at each section and their profile can change only along the reactor axis (z co-ordinate). In the development of the model it was also assumed that:

- the particles of the sorbents were spherical and uniformly distributed inside the reactor. The diameter of the particles was assumed equal to the average diameter of the granulometric distribution of the actual sorbent. Voidage inside the reactor, ε , was assumed constant;
- the solid was constituted by a mixture of three components: calcium oxide (CaO), magnesium oxide (MgO) and inert material. The solid composition was followed from the chemical analysis of the sorbent;

- the chemical reactions between gas and solid were:



The kinetic parameters for these reactions were chosen according to Arrhenius' law:

$$k_A = k_0 \exp\left(-\frac{E_a}{RT}\right) \quad (7)$$

- the reactions occurred throughout the solid particle where CO₂ transformed, continually and progressively, the CaO/MagO surface as long as "fresh" CaO/MgO surface was available. Therefore, each particle of the solid was considered an active site for the CO₂ absorption: inside the reactor $n(z,t)$ was the number of particles per unit area of solid at the coordinate z and at the generic time t . The volume of the particle available for the reaction was defined by the parameter R_c , which defined the spherical layer inside the particle that is inaccessible to the reaction (unreacted core);
- CO₂ absorption was described by a gas solid mass transfer coefficient according to the relationship valid for granular solid beds (Gianetto and Silveston 1986):

$$h = \left[\frac{G_o}{\rho S} + \frac{G_m}{\rho_m S} \right] \frac{2}{Y_o + Y_f} \frac{PM_A}{PM} \times \ln\left(1 - \frac{Y_o + Y_f}{2} \frac{PM}{PM_A}\right)^{-1} \frac{2.06 \text{Re}_p^{-0.575}}{\varepsilon \left(\frac{\eta}{\rho D_e}\right)^{0.67}} \quad (8)$$

The effective diffusivity D_e of the CO₂ through the particles was a function of the values of the tortuosity, the molecular diffusivity D_m , the Knudsen diffusion coefficient D_k and the porosity ε_x (Duo et al. 1993). According to (Hartman and Coughlin 1976,) the following correlation was adopted:

$$D_e = \frac{\varepsilon_x}{\tau} \left(\frac{1}{D_m} + \frac{1}{D_k} \right)^{-1} \quad (9)$$

3.2 Equations of the models

Since properties of the reaction mixture change only along the reactor length, the system was one-dimensional and the balance equations were referred to a cylindrical control volume included between two cross sections at z and $z+dz$. The balance equations considered in the model were:

Mass balance for CO₂ concentration

$$\frac{\partial C}{\partial t} = -\frac{u}{\varepsilon} \frac{\partial C}{\partial z} - \frac{a h k'_a n}{\varepsilon h + k'_a n} C \quad (10)$$

Balance of the solid particles number

$$\frac{\partial n}{\partial t} = -\frac{\Phi h k'_a n}{h + k'_a n} C \quad (11)$$

Energy balance for the gas

$$\frac{\partial T}{\partial t} = -\frac{u}{\varepsilon} \frac{\partial T}{\partial z} - \gamma(T - T_{so}) \quad (12)$$

where the coefficient γ was defined as:

$$\gamma = \frac{a h_T}{\varepsilon \rho C_p} \quad (13)$$

For the calculus of the heat transfer coefficient, h_T , the following correlation (Coulson and Richardson 1990) was used:

$$Nu_u = \frac{h_T d}{k} = 2 + 0.69 Re^{0.5} Pr^{0.33} \quad (14)$$

which is valid for spherical particles surrounded by a gas stream. The initial and boundary conditions for the equations (10), (11) and (12) were:

Equation (10):

$$C(z,0) = 0 \quad \forall z \neq 0, \quad C(z,0) = C_o \quad \text{if } z = 0,$$

$$C(0,t) = C_o \quad \forall t.$$

Equation (11):

$$n(z,0) = n_o$$

Equation (12):

$$T(z,0) = T_o \quad \forall z, \quad T(0,t) = T_o \quad \forall t.$$

The two partial differential equations (10) and (11) are coupled. Finite difference techniques were employed to carry out the numerical integration system of equations (10), (11) and (12) using MATLAB software (Borse 1996, Demidovic and Maron 1981).

Figure 6 shows the typical gas temperature profiles inside the reactor obtained by solving equation (12) at two different solid bed temperatures, 100°C and 200°C, respectively. From the Figure, it is evident that the gas temperature reaches the solid bed temperature after a few centimetres inside the reactor.

Therefore, at each time the gas temperature inside the reactor can be considered practically constant and equal to the solid bed temperature.

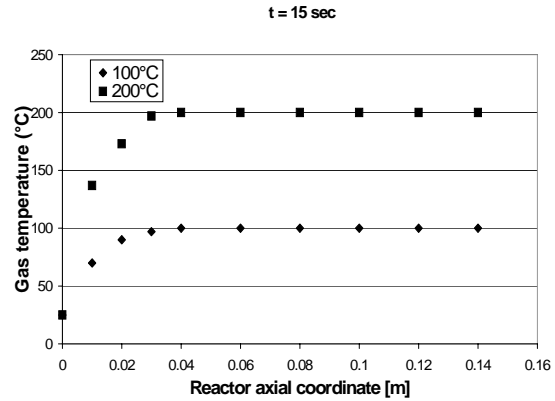


Figure 6. Typical gas temperature profiles inside the reactor at two different temperatures of the solid bed at time $t = 15$ s

4. Application of the Model to the Experimental Data

The kinetic parameters obtained in the Arrhenius Plot for the CaO/CO₂ reaction (Figure 5) were also applied in the mathematical model, in a rough approach, for MgO/CO₂ reaction, together with the chemical composition and physical properties of the solid sorbents shown in TABLE II. Moreover, the flow and chemical composition of the gas inlet to the reactor were fixed according to the values of TABLE I. In Figure 7, CO₂ concentration profiles at the outlet of the reactor for the blast furnace slag at two different temperatures (100°C and 200°C) are compared with the corresponding model results. The agreement between the experimental data and theoretical prediction is good. Figure 8 shows, for the CaO, the CO₂ specific absorption at different temperatures comparing the experimental results with the model's predictions. As expected, there is a good agreement between the experimental and model results.

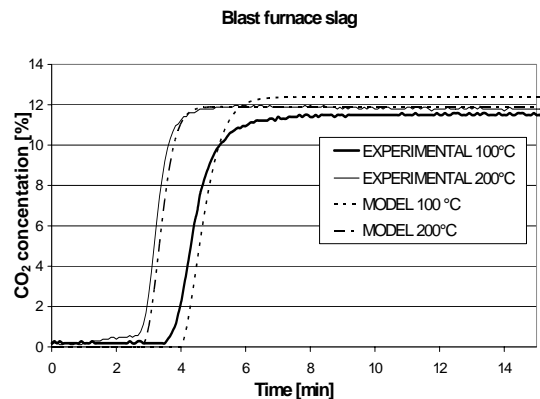


Figure 7. CO₂ concentration profile at the outlet of the reactor: a comparison between experimental and model results

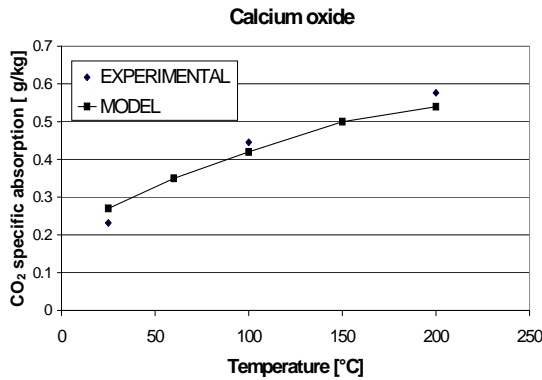


Figure 8. CO_2 specific absorption at different temperatures for the CaO: a comparison between experimental and model results

Finally, a quantitative comparison of the model predictions with the experimental results is shown in TABLE III. Here again it is evident that the theory quite satisfactorily predicts the experimental results.

TABLE III. QUANTITATIVE COMPARISON OF THE MODEL PREDICTIONS WITH THE EXPERIMENTAL RESULTS

	Calcium Oxide					
	EXPERIMENTAL			MODEL		
	25 °C	100 °C	200 °C	25 °C	100 °C	200 °C
CO_2 removal efficiency [%]	8	15.4	19.9	9.4	12.76	14.36
CO_2 stationary removal efficiency [%]	2.2	4.28	8.2	3.2	7.38	14.39
CO_2 specific absorption [g/kg]	0.23	0.45	0.58	0.27	0.42	0.54
Rate constant per surface reaction [m/s]	9.19E-08	4.24E-07	6.67E-07	1.10E-07	3.44E-07	9.67E-07
	Blast Furnace Slag					
	EXPERIMENTAL			MODEL		
	25 °C	100 °C	200 °C	25 °C	100 °C	200 °C
CO_2 removal efficiency [%]	13.7	11.5	10.0	6.8	7.8	11.4
CO_2 stationary removal efficiency [%]	6.8	6.0	6.6	1.4	3.3	7.7
CO_2 specific absorption [g/kg]	0.61	0.44	0.38	0.26	0.30	0.43
Rate constant per surface reaction [m/s]	8.49E-08	5.84E-08	5.75E-08	1.02E-08	3.53E-08	9.94E-08
	Coal Bottom Ash					
	EXPERIMENTAL			MODEL		
	25 °C	100 °C	200 °C	25 °C	100 °C	200 °C
CO_2 removal efficiency [%]	6.0	5.3	4.1	2.6	2.6	3.0
CO_2 stationary removal efficiency [%]	3.5	3.3	3.5	0.1	0.4	0.9
CO_2 specific absorption [g/kg]	0.14	0.12	0.1	0.05	0.05	0.06
Rate constant per surface reaction [m/s]	5.17E-09	4.92E-09	7.14E-09	8.15E-10	2.86E-09	8.09E-09
	Limestone					
	EXPERIMENTAL			MODEL		
	25 °C	100 °C	200 °C	25 °C	100 °C	200 °C
CO_2 removal efficiency [%]	7.0	5.5	5.3	3.0	5.2	8.3
CO_2 stationary removal efficiency [%]	2.0	2.0	2.0	1.1	3.2	6.7
CO_2 specific absorption [g/kg]	0.19	0.15	0.14	0.10	0.16	0.26
Rate constant per surface reaction [m/s]	6.96E-08	6.38E-08	7.88E-08	1.99E-08	6.83E-08	1.92E-07

5. Conclusions

The bottom ash and the limestone show a low CO_2 removal efficiency (lower than 7%), which is practically constant with the temperature. The blast furnace slag and, especially, the CaO show, in the range of temperatures investigated an appreciable CO_2 removal efficiency (8%-20% for the CaO, 10%-14% for the blast furnace slag). It is important to stress that the CO_2 specific absorption measured is very low for all sorbents examined (lower than 1 gm of CO_2 absorbed for 1 kg of solid). For this reason, the application of this gas-solid absorption process to a typical thermal power plant in order to obtain significative reduction in the CO_2 emission, with the materials considered in this paper is not feasible due to the enormous

amounts of solid that should be necessary for this purpose. Indeed, for example, if this process is applied in a 320 MWe coal-fired power plant, in order to obtain a CO_2 emission reduction of 10%, using particles of CaO with a diameter equal to 1 mm and a flue gas velocity equal to 2 m/s, four isothermal reactors in parallel configuration ($T=300^\circ\text{C}$) with a diameter and length equal to 10 m and 300 m, respectively, should be adopted.

The predictions of the mathematical model used in order to study the CO_2 absorption inside the reactor are in good agreement with the experimental results. In conclusion, the developed model is an effective tool to study the gas-solid absorption in a wide range of CO_2 concentration, sorbent particles' size and temperature.

Nomenclature

a	reaction interfacial area per unit volume of sorbent particles [m^2/m^3]
C	CO_2 concentration [kg/m^3]
C_o	CO_2 inlet concentration [kg/m^3]
C_p	gas specific heat at constant pressure [$\text{J}/\text{kg}/\text{s}$]
d	average diameter of the particles [m]
u	gas velocity [m/s]
D_e	effective diffusivity of CO_2 [m^2/s]
D_m	molecular diffusion coefficient [m^2/s]
D_k	Knudsen diffusion coefficient [m^2/s]
E_a	activation energy [kJ/mole]
G_o	inlet gas mass flow rate [kg/s]
G_m	inlet particulate matter mass flow rate [kg/s]
H	length of the reactor [m]
h	mass transfer coefficient [m/s]
h_T	heat transfer coefficient [$\text{J}/\text{m}^2/\text{K}/\text{s}$]
k	conductivity of reactant gas [$\text{J}/\text{m}^2/\text{K}/\text{s}$]
k_A	rate constant per surface reaction [m/s]
k'_a	apparent rate constant ($k'_a = \pi d^2$) [m^3/s]
k_o	pre-exponential factor [m/s]
M	weight of the sorbent inside the reactor [kg]
Nu	Nusselt number [-]
n	number of particles per unit area of solid [m^{-2}]
n_o	initial number of particles per unit area of solid [m^{-2}]
Pr	Prandtl number [-]
PM_A	CO_2 molecular weight [kg/kmol]
PM	gas molecular weight [kg/kmol]
Re	Reynolds number [-]
Q_o	inlet gas flow rate [m^3/s]
R	universal gas constant [J/mol/K]
R_p	particle Reynolds number [-]
R_c	unreacted core radius [m]
S	cross-sectional area of the reactor [m^2]
T	gas temperature [K]
T_{so}	reactor temperature [K]

T_o	gas inlet temperature [K]
t_r	duration of experimental test [s]
u	gas velocity [m/s]
$v(t)$	CO ₂ absorption rate at time t [kg/s]
Y_o	inlet CO ₂ mass fraction [-]
Y_f	outlet CO ₂ mass fraction [-]
γ	coefficient in eq. 13 [-]
ε	interparticles voidage [-]
ε_x	porosity of reacting particles [-]
θ	particle's shape factor $\theta = 6/d$ [m ⁻¹]
η	gas viscosity [kg/m /s]
ρ	gas density [kg/m ³]
ρ_m	particulate density [kg/m ³]
τ	tortuosity [-]
Φ	converted particles per unit mass of CO ₂ absorbed [kg ⁻¹]

References

- Bacci, P., 2001, "Problematiche Fisiche Relative all'Effetto Serra", *Giornale di Fisica*, Vol.XVLII, No. 1, pp. 3-13.
- Bhatia, S.K., Perlmutter, D.D., 1983, "Effect of the Product Layer on the Kinetics of the CO₂-Lime Reaction", *AIChE Journal*, Vol.29, No.1, pp.79-86.
- Borse, G.J., 1996, *Numerical Methods with MATLAB*, PWS Publishing Company, Boston.
- Coulson, J.M., Richardson J.F., 1990, *Chemical Engineering, Volume I.*, Pergamon Press, Oxford.
- Davison, J., Freund, P., Smith, A., 2001, "Putting Carbon Back into the Ground", report no. ISBN 1898373280, IEA Greenhouse Gas R&D Programme, Cheltenham, UK.
- Dedman, A.J., Owen, A.J., 1962, "Calcium Cyanamide Synthesis: the Reaction $\text{CaO} + \text{CO}_2 = \text{CaCO}_3$ ", *Trans. Faraday Soc.*, No. 58, pp. 2027-2035.
- Demidovic, B.P., Maron, I.A., 1981, *Fondamenti di Calcolo Numerico*, Edizioni Mir, Genova, Italy.
- Duo, W., Seville, J.P.K., Kirkby, N.F., Clift, R., 1993, "Prediction of Dry Scrubbing Process Performance" *Gas Cleaning at High Temperatures*, pp 644-662.
- Gianetto, A., Silveston, P.L., 1986, *Multiphase Chemical Reaction. Theory, Design, Scale-Up*, Springer Verlag, Berlin.
- Giavarini, C., Maccioni, F., 2001, "Lo Stoccaggio della CO₂ negli Oceani", *La Chimica e l'Industria*, No. 83, pp. 1-4.
- Gupta, H., Jadhav, R., Fan, L.S., 2001, "CO₂ Separation from Flues Gas by the Carbonation and Calcination of Metal Oxides", report no.Project C1.11, www.ohiocoal.org/projects/Year1/c111.pdf, Ohio State University, 2001, Columbus.
- Hartman, H., Coughlin, R.W., 1976, "Reaction of Sulfur Dioxide with Limestone and the Influence of Pore Structure", *Ind. Eng. Chem. Process Des. Develop.*, Vol. 13, No. 3, pp. 248-253.
- Levenspiel, O., 1978, *Chemical Reaction Engineering*, Casa Editrice Ambrosiana, Milano, Italy.
- Liro, C.R., Adams, E.E, Herzog, H.J., 1992, "Modelling the Release of CO₂ in the Deep Ocean" *Energy Convers. Mgmt*, No. 33, pp. 667-674.
- Mess, D., Sarofim, A.F., Longwell, J.P., 1999, "Product Layer Diffusion during the Reaction of Calcium Oxide with Carbon Dioxide", *Energy & Fuels*, No. 13, pp. 999-1005.
- Ormerod, W.G., Freund, P., Smith, A, 2002, "Ocean Storage of CO₂", report No. ISBN 1898373302, IEA Greenhouse Gas R&D Programme, Cheltenham, UK
- Reeve, D.A., 2001, "The Capture and Storage of Carbon Dioxide Emissions", report no. M92-211, Natural Resources Canada, Office of Energy Research and Development, Ottawa, Ontario, Canada.
- Sigman, D.M., Boyle, E.A., 2000, "Glacial interglacial variations in atmospheric carbon dioxide", *Nature*, Vol. 407, No.,19, pp. 859-869.